THE JOURNAL OF PHYSICAL CHEMISTRY C LETTERS

**2009,** *113,* 15102–15105
Published on Web 08/03/2009

# Water Nucleation on Gold: Existence of a Unique Double Bilayer

**D. Stacchiola,[†,§] J. B. Park,[†,⊥] P. Liu,[†,‡] S. Ma,[†,#] F. Yang,[†] D. E. Starr,[‡] E. Muller,[‡] P. Sutter,[‡] and J. Hrbek*[,†]**

*Chemistry Department, Brookhaven National Laboratory, Upton, New York 11973, Center for Functional Nanomaterials, Brookhaven National Laboratory, Upton, New York 11973, Department of Chemistry, Michigan Technological University, Houghton, Michigan 49931, Institute of Fusion Science, Department of Chemistry Education, Chonbuk National University, Jeonju, Jeonbuk, 561-756 South Korea, and College of Engineering and Computing, University of South Carolina, Columbia, South Carolina 29208*

*Received: May 25, 2009; Revised Manuscript Received: July 21, 2009*

Combining the results from experimental (STM and IRAS) and theoretical (DFT) studies of water adsorption on gold, we show that the Au(111) surface is hydrophobic. The weak interaction of water with Au induces the formation of a unique double bilayer, which itself is hydrophobic due to the internal locking of all hydrogen bonds within the bilayer and between the two bilayers of the water clusters.

## Introduction

Liquid−solid interfaces, particularly the interaction of water with surfaces, have far-reaching consequences in physical and biological sciences[1] and play a significant role in technology.[2,3] After years of research, a molecular-level understanding of the physical properties determining the structure of water at a wide range of interfaces is beginning to emerge.[4] Thermodynamically, the wettability of a surface is determined by the relative energies of the various interfaces (solid−vapor, solid−liquid, and liquid−vapor) formed when water is condensed on the surface. Recent research has largely focused on the molecular structure of water during the initial stages of condensation. The results have demonstrated that the molecular structure of the first water layer adsorbed on a surface governs its wetting properties.[5] In turn, this controls the chemical and physical properties of surfaces in technologically relevant processes such as catalysis and corrosion. However, even for simple model systems such as close-packed metal surfaces, there are still opened questions about the transition from adsorbed water molecules at the initial stages of liquid−solid interface formation[6] to the formation of water clusters and eventually ice layers.

A unique property of water molecules is their ability to form strong directional hydrogen bonds, which are responsible for molecular aggregation and formation of amorphous solid water (ASW) or crystalline solid ice on substrates, depending on the conditions used during the growth of water films.[7] The most common hexagonal phase of bulk ice has low density and consists of layered sheets of puckered water hexamers. In the basal plane, a water molecule has a staggered arrangement of hydrogen bonding with respect to three of its neighbors, while its fourth neighbor has an eclipsed hydrogen bond that holds the hexamer sheets together. Water molecules adsorbed on most metal surfaces form ice-like puckered (often called bilayer, BL) hexamers, with vertical displacements dependent on the electronic and geometrical structures of the substrate.[4] The effect of the substrate can extend beyond the first BL and affect the water structure of second and additional BLs, thus modifying their wettability.

Water ice layers formed on metal surfaces are used for the preparation of supported metal[8] and oxide[9,10] nanoparticles. Titania nanoparticles grown by water reactive-layer-assisted deposition on a Au(111) surface form an array that replicates the underlying herringbone reconstruction of the substrate.[9] To understand the impact of the water buffer on the structure of the formed nanoparticles, it is important to address the wettability of clean gold surfaces by water. On the basis of experimental results from several techniques, contradicting claims have appeared in the literature which have not yet been resolved; gold is claimed to be hydrophobic[7] or hydrophilic.[11] Recent theoretical studies have proposed that gold surfaces should be hydrophobic.[12]

We present here a combined experimental and theoretical study of the adsorption and nucleation of water on Au(111) using infrared reflection absorption spectroscopy (IRAS), scanning tunneling microscopy (STM), and density functional theory (DFT) calculations. The results show that gold is, in effect, hydrophobic and that through the formation of intrahydrogen bonding inside of water clusters and as a result of the weak interaction of water with gold, unique double bilayer structures are formed as precursors to the formation of 3D ice clusters.

## Experimental and Computational Details

The experiments were performed in an ultrahigh vacuum (UHV) chamber (with a base pressure below $1 \times 10^{-10}$ mbar) interfaced with an IFS 66v Bruker spectrometer for IRAS and standard facilities for sample preparation. The IRAS spectra were measured with p-polarized light at an 84° grazing angle of incidence (with a resolution of 4 $cm^{-1}$). The low-temperature STM images were obtained in a separate UHV instrument at

* To whom correspondence should be addressed. E-mail: hrbek@bnl.gov.
† Chemistry Department, Brookhaven National Laboratory.
‡ Center for Functional Nanomaterials, Brookhaven National Laboratory.
§ Michigan Technological University.
⊥ Chonbuk National University.
# University of South Carolina.

10.1021/jp904875h CCC: $40.75 

the Center for Functional Nanomaterials. This chamber is a multitechnique (XPS, ISS, LEED) surface analysis chamber equipped with an RHK UHV-700 variable-temperature STM with cooling capabilities down to <20 K and heating to >1500 K. High sample bias and low tunneling currents were used to minimize modification of the water clusters while scanning.[13] High-purity $D_2O$ (99.96%), dosed by backfilling the chambers, was used for the IRAS experiments to facilitate the distinction between the adsorption of molecules at the surface and small changes in the absorption of $H_2O$ in the IR optical path.

The unrestricted DFT calculations were performed using the DMol$^3$ code.[14,15] The ionic cores were described by effective core potentials. A numerical basis set was used with comparable accuracy to a Gaussian 6-31G (d) basis set. A local basis cutoff of 5.0 Å in real space was employed. The generalized gradient approximation with the PW91 functional[16] was utilized in the present work. To model the Au(111) surface, we followed the supercell approach with two-layer slabs with a 3 × 3 surface unit cell and a 15 Å vacuum between the slabs. Nine k-points were selected for the surfaces. The adsorption of puckered water BLs in the $(\sqrt{3} \times \sqrt{3})R30°$ symmetry on Au(111) was calculated. The top layer of the surfaces was allowed to fully relax with water molecules present. Due to the weak interaction between Au(111) and water, increasing the number of Au layers up to four did not make significant change in the adsorption energy of water (<0.02 eV/$H_2O$). The adsorption energy for an adsorbed water structure ($E$) was expressed as the mean adsorption energy per molecule, $E = [E(nH_2O/Au) - E(Au) - nE(H_2O)]/n$. Here, $E(nH_2O/Au)$ is the total energy of the adsorption system, $E(H_2O)$ and $E(Au)$ are energies of the free water molecule and the Au(111) surface, respectively, and $n$ is the number of water molecules in the cell.

## Results and Discussion

Results of recent STM experiments have shown that during the initial stage of water adsorption on Au(111) (<0.01 ML) and at very low temperatures (~5 K), monomers are trapped at the elbows of the herringbone reconstruction of the surface.[17] To investigate subsequent water cluster nucleation, we dosed small amounts of water (0.04−3 ML) at slightly higher temperatures to facilitate molecular diffusion. A STM image after the exposure of 0.04 L (1 L = 1 × $10^{-6}$ mbar s) of water at 20 K is presented in Figure 1A. At this temperature, water still diffuses and nucleates preferentially at the elbow sites. Due to the weak interaction of water with gold and the formation of interlocked water structures through hydrogen bonding, special consideration has to be taken for the STM scanning parameters in order to limit tip-induced damage of adsorbed structures. Following the findings of a recent report where water multilayers were imaged on Pt(111),[13] negative bias and low currents (−5 ± 1 V, 3−5 pA) were applied during all of the STM experiments reported here. A bimodal distribution of cluster heights was observed, with apparent mean heights of 0.11 ± 0.01 and 0.18 ± 0.01 nm (Figure 1). The total area covered by water clusters was 0.07 ML. When the water exposure was increased, the main effect observed was a corresponding increase in the density of clusters with an average height of 0.18 nm and the disappearance of small clusters. Figure 1B shows a STM image after exposure of 0.5 L of water. Even at this stage, where most of the elbows are occupied by water islands with an average 0.19 ± 0.04 nm height, the bare Au surface can still be observed in between the islands, clearly demonstrating the lack of a wetting water layer on the Au(111) surface.

The STM images in Figure 1 show that water nucleates in small clusters predominantly at the elbows of the herringbone

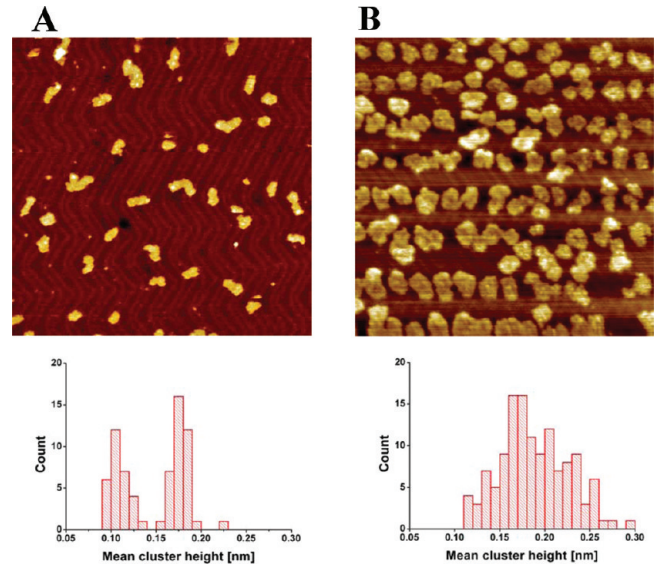


**Figure 1.** STM images (100 × 100 nm, −6 V, 4 pA) and corresponding histograms of adsorption of water on Au(111) at 20 K (A) after exposure to 0.04 L of $H_2O$ (area fraction covered: 0.07) and (B) after exposure to 0.5 L of $H_2O$ (area fraction covered: 0.38).

reconstruction. The apparent heights (~0.1 nm) of these small clusters are consistent with those reported for single water bilayers adsorbed on other metals surfaces.[18] As the water exposure is increased, the clusters form structures with an apparent height twice (~0.2 nm) that of single bilayers, suggesting the formation of double bilayer structures. Since STM measured heights cannot, in general, be directly correlated to geometrical heights, we have investigated the stability of double bilayer water structures on Au(111) theoretically.

DFT calculations were employed to investigate early stages of water adsorption on Au(111). The adsorptions of 1 BL, 2 BLs, and 3 BLs of water were each explored in our calculations. The water adsorption energy and the corresponding geometries are plotted in Figure 2A. For 1 BL water adsorption on Au(111), there are two possibilities, having hydrogen atoms pointing up (H-up) or down (H-down). In agreement with previous calculations,[12] our results show that the two structures are very close in energy, with the H-down configuration slightly more stable than the H-up configuration by 0.04 eV/$H_2O$. In the case of the 2 BL structure, three different structures were considered with H-up for both water layers (H-up|H-up), H-down for both water layers (H-down|H-down), and H-up for the bottom water layer and H-down for the top water layer (H-up|H-down). Our results indicate that the stability of these structures decreases in the sequence H-up|H-down (−0.69 eV/$H_2O$; see Figure 2A) > H-down|H-down (−0.60 eV/$H_2O$) > H-up|H-up (−0.53 eV/$H_2O$). Therefore, the structure with all hydrogen locked in the two water layers is the most stable, enhancing the stability per water molecule by ~0.15 eV with respect to the 1 BL structure. In addition, according to our calculations, the transition from the H-down|H-down to the H-up|H-down structure is very facile, with a barrier of only 0.06 eV. That is, H-up|H-down will form regardless of which 1 BL structure the water adopts, either H-up or H-down. The formation of intralayer hydrogen bonding with ~0.3 eV per bond is also more favorable than the interaction of the bottom water molecules with Au (~0.1 eV). The 2 BL structure described here is similar to a bilayer ice phase confined in pores that was proposed theoretically.[19]

By adding one more BL, the structures in both H-up(bottom water layer)|H-down(middle layer)|H-down(top water layer) and

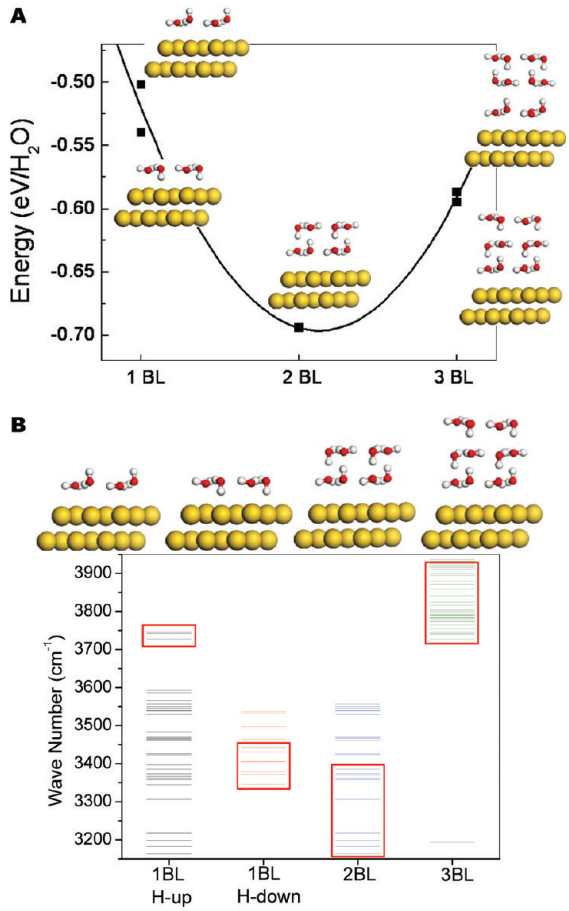


**Figure 2.** (A) DFT-calculated adsorption energies for water multilayers adsorbed on Au(111). The figures show the corresponding optimized geometries (yellow: Au; red: O; white: H). (B) Bottom: Calculated vibrational frequencies for water adsorption on Au(111). Top: Corresponding geometries. The frequencies framed by rectangles correspond to modes perpendicular to the surface.

H-up|H-up|H-down are energetically similar. However, none of the 3 BL structures can lock hydrogen internally in the cluster in the same way as the 2 BL structure, where each oxygen atom has four hydrogen atoms coordinated to it. The growth of the third water BL on Au(111) always results in some of the oxygen atoms coordinated to three hydrogen atoms (Figure 2A). As a result, the 3 BL structures are not energetically preferred and are less stable than the 2 BL clusters by ~0.1 eV/$H_2O$, although they remain marginally more stable than 1 BL clusters (Figure 2A). Overall, our DFT calculations demonstrate that when increasing the water coverage from 1 BL to 3 BL, the 2 BL structure (H-up|H-down) is energetically favored on Au(111), in agreement with the STM observations (Figure 1).

Since the geometrical heights cannot unequivocally be established from STM measurements, as mentioned above, and the clusters may potentially be modified during the scanning process,[13] we looked for confirmation of the 2 BL clusters' existence using IR spectroscopy. Figure 2B presents the DFT-calculated IR spectrum of the different structures. The frequencies framed by rectangles correspond to the O−H stretch modes perpendicular to the surface. Due to the multitude of modes, broad features are predicted. Nevertheless, we can clearly differentiate between 2 BL and 3 BL structures by the absence or presence of features in the O−H stretch region above 3700 $cm^{-1}$. The O−H stretch with the hydrogen atoms locked in between two BLs of water (2 BL, Figure 2B) displays lower frequencies than those with H-atoms pointing toward the gold

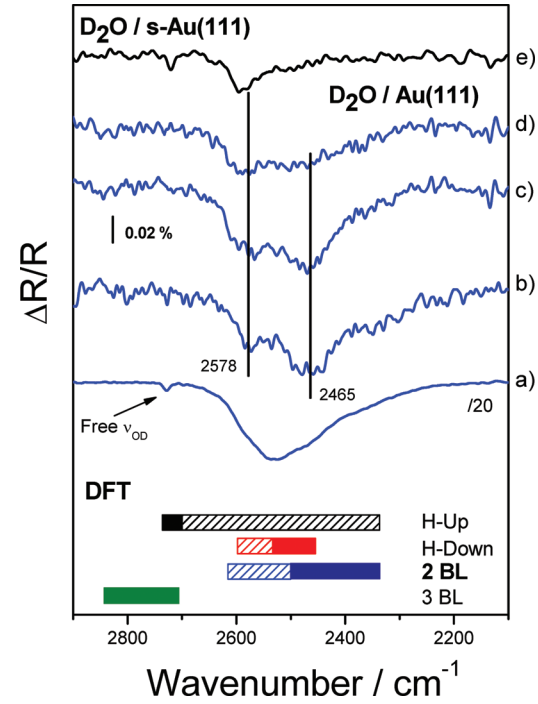


**Figure 3.** IRAS spectra of $D_2O$ adsorbed on Au(111); the ASW multilayer on a well-ordered Au(111) surface (curve a) is transformed, after desorption, to crystalline water clusters without free O−D bonds (curves b−d), while the free O−D stretch is visible on a rough Au(111) surface (curve e).

substrate (1 BL H-down) or the vacuum (1 BL H-up) and also than those from the two configurations of 3 BLs of water.

The IRAS technique is well-suited for studies of the orientation of adsorbed molecules on metal surfaces and of the interactions between the metal surface and adsorbed molecule as well as intermolecular interactions within an adsorbed layer.[20] Two $\nu_{OD}$ stretching modes in IRAS spectra associated with hydrogen bonding were previously reported at ~2470 and ~2570 $cm^{-1}$ for low-coverage $D_2O$ adsorption on Pt(111)[21] and Rh(111).[22] The third peak present at ~2700 $cm^{-1}$ in the spectra was assigned to the O−D stretching vibrations of $D_2O$ with an O−D bond pointing up, that is, free or dangling O−D bonds of the water cluster.[23] To obtain IR data of small water clusters, we adsorbed a water multilayer and slowly annealed the sample while recording the spectra of the surface-bound water. Figure 3 shows selected IRAS spectra of $D_2O$ adsorbed on Au(111) measured at 110 K. The thick water multilayer spectrum (curve a) measured without annealing is a typical IR spectrum of amorphous solid water.[24] It is dominated by a strong asymmetric stretching mode at ~2535 $cm^{-1}$ and a second weaker but still clearly visible mode at ~2720 $cm^{-1}$. Annealing transforms ASW to crystalline ice that is characterized by much sharper $\nu_{OD}$ stretching modes[22] (data not shown). Additional annealing leads to water desorption, and spectra b−d correspond to water in the submonolayer coverage range. Two weak broad features were observed at 2465 and 2578 $cm^{-1}$, but no mode was detected in the region of dangling O−D bonds. Interestingly, upon adsorption of water on top of a rough-sputtered Au surface (curve e), a broad mode at ~2580 $cm^{-1}$ is accompanied by a weaker mode in the O−D stretch region at ~2720 $cm^{-1}$. IRAS is sensitive enough to detect free O−D at very low coverages on a rough surface, and we conclude that the dangling O−D bonds are not present on low-coverage water layers grown on a well-ordered Au(111) surface.

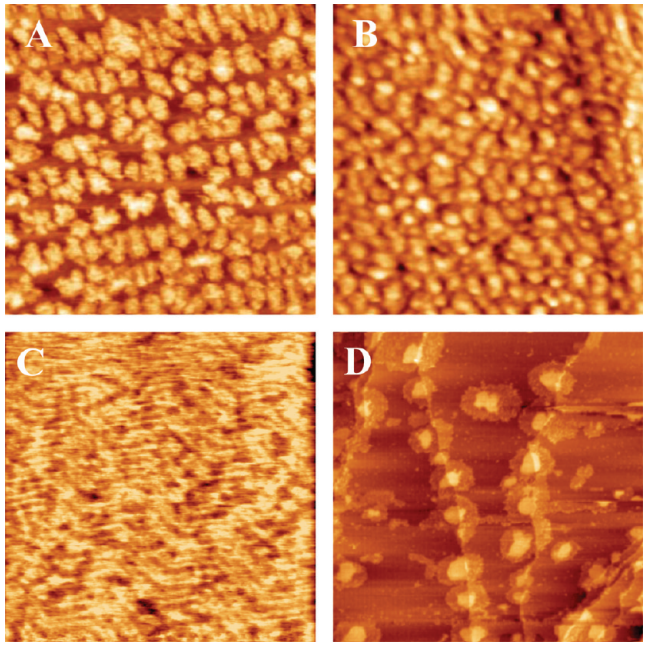


**Figure 4.** STM images of water clusters adsorbed on Au(111) after adsorption of (A) 1.0 L of $H_2O$ at 20 K (average height: ~0.3 nm; image size: 100 × 100 nm), (B) 3.0 L of $H_2O$ at 20 K (rough surface with peaks up to 0.7 nm in height; image size: 100 × 100 nm), (C) 0.2 L of $H_2O$ adsorbed and imaged at 100 K (image size: 100 × 100 nm), and (D) 1.5 L of $H_2O$ at 120 K (images taken at 20 K; image size: 300 × 300 nm).

The DFT-calculated frequencies for different types of clusters (see Figure 2B) adjusted by their corresponding isotopic effect are shown at the bottom of Figure 3. The vibrational analysis helped us to exclude the presence of clusters with three or more BL at low water coverages, supporting the results of STM and DFT that suggest that 2 BL clusters are preferentially formed on Au(111) at low coverages of water.

After exposing the Au(111) surface to 1 L of water at 20 K, the bare Au surface in between the water clusters can still be observed, but clusters start to grow higher than 0.2 nm (Figure 4A). By 3.0 L of exposure to water, the surface is completely covered, and 3D clusters are clearly observed (Figure 4B). When water is adsorbed and imaged at 100 K (Figure 4C), as originally done by Ikemiya and Gewirth,[11] imaging becomes difficult due to the high mobility of water and tip-induced effects, and consequently, the morphology of the observed structures changes from image to image. The STM image shown in Figure 4D was obtained by dosing 1.5 L of water at 120 K and then scanning at 20 K. The first step of the multistep "hat-shaped" clusters has the height of the double bilayer. The clusters observed at these temperatures are nucleating from step edges and form extended clusters instead of nucleating at the elbows of the herringbone reconstruction and forming small clusters, as observed during the adsorption of water at lower temperatures.[17]

In summary, the results of the combined STM, DFT, and IRAS investigation presented here support both the original proposal by Smith et al.[7] and later theoretical results[12] that Au(111) is hydrophobic in character. In addition, the data are consistent with the weak interaction of water with Au that leads to a unique double bilayer formation, which itself is hydrophobic due to the internal locking of hydrogen bonds in the water clusters.

**Acknowledgment.** Both experiments and calculations were carried out at the Department of Chemistry and the Center for Functional Nanomaterials of Brookhaven National Laboratory, and the research was supported by the U.S. DOE, Chemical Sciences Division, Grant No. DE-AC02-98CH10886.

## References and Notes

(1) Granick, S.; Bae, S. C. *Science* **2008**, *322*, 1477.
(2) Thiel, P. A.; Madey, T. E. *Surf. Sci. Rep.* **1987**, *7*, 211.
(3) Henderson, M. A. *Surf. Sci. Rep.* **2002**, *46*, 5.
(4) Verdaguer, A.; Sacha, G. M.; Bluhm, H.; Salmeron, M. *Chem. Rev.* **2006**, *106*, 1478.
(5) Yamamoto, S.; Andersson, K.; Bluhm, H.; Ketteler, G.; Starr, D. E.; Schiros, T.; Ogasawara, H.; Pettersson, L. G. M.; Salmeron, M.; Nilsson, A. *J. Phys. Chem. C* **2007**, *111*, 7848.
(6) Carrasco, J.; Michaelides, A.; Forster, M.; Haq, S.; Raval, R.; Hodgson, A. *Nat. Mater.* **2009**, *8*, 427.
(7) Smith, R. S.; Huang, C.; Wong, E. K. L.; Kay, B. D. *Surf. Sci.* **1996**, *367*, L13.
(8) Palmer, J. S.; Sivaramakrishnan, S.; Waggoner, P. S.; Weaver, J. H. *Surf. Sci.* **2008**, *602*, 2278.
(9) Song, D.; Hrbek, J.; Osgood, R. *Nano Lett.* **2005**, *5*, 1327.
(10) Kaya, S.; Sun, Y. N.; Weissenrieder, J.; Stacchiola, D.; Shaikhutdinov, S.; Freund, H. J. *J. Phys. Chem. C* **2007**, *111*, 5337.
(11) Ikemiya, N.; Gewirth, A. A. *J. Am. Chem. Soc.* **1997**, *119*, 9919.
(12) Meng, S.; Wang, E. G.; Gao, S. W. *Phys. Rev. B* **2004**, *69*, 195404.
(13) Thurmer, K.; Bartelt, N. C. *Phys. Rev. B* **2008**, *77*, 195425.
(14) Delley, B. *J. Chem. Phys.* **1990**, *92*, 508.
(15) Delley, B. *J. Chem. Phys.* **2000**, *113*, 7756.
(16) Perdew, J. P.; Wang, Y. *Phys. Rev. B* **1992**, *45*, 13244.
(17) Gawronski, H.; Morgenstern, K.; Rieder, K. H. *Eur. Phys. J. D* **2005**, *35*, 349.
(18) Morgenstern, K.; Rieder, K. H. *J. Chem. Phys.* **2002**, *116*, 5746.
(19) Koga, K.; Zeng, X. C.; Tanaka, H. *Phys. Rev. Lett.* **1997**, *79*, 5262.
(20) Hoffmann, F. M. *Surf. Sci. Rep.* **1983**, *3*, 107.
(21) Nakamura, M.; Shingaya, Y.; Ito, M. *Chem. Phys. Lett.* **1999**, *309*, 123.
(22) Beniya, A.; Sakaguchi, Y.; Narushima, T.; Mukai, K.; Yamashita, Y.; Yoshimoto, S.; Yoshinobu, J. *J. Chem. Phys.* **2009**, *130*, 034706.
(23) Rowland, B.; Devlin, J. P. *J. Chem. Phys.* **1991**, *94*, 812.
(24) Haq, S.; Hodgson, A. *J. Phys. Chem. C* **2007**, *111*, 5946.

JP904875H